



**HAL**  
open science

## **A new urban soil model for SOLENE-microclimat: Review, sensitivity analysis and validation on a car park**

Marie-Hélène Azam, Benjamin Morille, Jérémy Bernard, Marjorie Musy,  
Fabrice Rodriguez

### ► **To cite this version:**

Marie-Hélène Azam, Benjamin Morille, Jérémy Bernard, Marjorie Musy, Fabrice Rodriguez. A new urban soil model for SOLENE-microclimat: Review, sensitivity analysis and validation on a car park. *Urban Climate*, 2017, 10.1016/j.uclim.2017.08.010 . hal-01629430v1

**HAL Id: hal-01629430**

**<https://hal.science/hal-01629430v1>**

Submitted on 6 Nov 2017 (v1), last revised 1 Jun 2018 (v2)

**HAL** is a multi-disciplinary open access archive for the deposit and dissemination of scientific research documents, whether they are published or not. The documents may come from teaching and research institutions in France or abroad, or from public or private research centers.

L'archive ouverte pluridisciplinaire **HAL**, est destinée au dépôt et à la diffusion de documents scientifiques de niveau recherche, publiés ou non, émanant des établissements d'enseignement et de recherche français ou étrangers, des laboratoires publics ou privés.

# Urban soil model under summer conditions: review, sensitivity analysis and validation

AZAM Marie-Hélène<sup>a,\*</sup>, MORILLE Benjamin<sup>a</sup>, BERNARD Jérémy<sup>a,b</sup>,  
MUSY Marjorie<sup>a,c</sup>, RODRIGUEZ Fabrice<sup>a,d</sup>

*Nantes, FRANCE*

<sup>a</sup>*Institut de Recherche en Sciences et Techniques de la Ville, FR CNRS 2488, France*

<sup>b</sup>*UMR AAU – CRENAU, Ecole Nationale Supérieure d'Architecture de Nantes – 6 quai  
François Mitterrand – BP 16202, F-44262 Nantes cedex 2, France*

<sup>c</sup>*Cerema Ouest, 9 rue René Viviani, 44000 Nantes, France*

<sup>d</sup>*Institut français des sciences et technologies des transports, de l'aménagement et des  
réseaux, France*

---

## Abstract

The main purpose of this study is to propose a model that well reproduces the heat storage flux into urban ground as well as surface temperature evolution. For that purpose a complete bibliographic review is first achieved. Some lacks are identified and the methodology to define the model in agreement with the conclusions of the literature review is presented as well as the way to assess its performances. Three nodes distributions are proposed regarding ground temperature profiles using an analytic solution. A sensitivity study is achieved on a large number of parameters: the material properties, the size of the layers, the deep boundary condition, and the convective heat transfer coefficient. The model ability to reproduce heat conduction transfer is validated thanks to a measurement campaign realized on a large asphalt

---

\*Corresponding author. E-mail address: marie-helene-azam@hotmail.fr Address: Cerema Ouest, 9 rue René Viviani, 44000 Nantes, France

parking lot during two clear and hot days. The RMSE between estimated and observed surface temperature is  $0.75^{\circ}C$ . The validation also include comparison with temperature at 4 different depths. The RMSE are  $0.73^{\circ}C$ ,  $0.48^{\circ}C$ ,  $0.21^{\circ}C$  and  $0.06^{\circ}C$  respectively at 5cm, 10cm, 34cm and 50cm. Performances obtained with the model using different nodes distributions are discussed and compared with results from the literature. The model presents better performances than most of others models applied in quite similar conditions. Finally, the application of the proposed model at a yearly scale demonstrates that the accuracy loss caused by the decrease of the nodes number depends on weather conditions. In particular, the most difficult days to simulate are clear and sunny days.

*Keywords:* Urban soil model, Heat transfer, Soil surface temperature, SOLENE-Microclimat.

---

## Contents

<b>1</b>	<b>Introduction</b>	<b>3</b>
<b>2</b>	<b>State of the art</b>	<b>5</b>
2.1	Existing models . . . . .	5
2.2	Parametrization of finite differences models . . . . .	9
<b>3</b>	<b>Methodology of the study</b>	<b>13</b>
3.1	Proposed soil model . . . . .	13
3.1.1	Deep boundary condition . . . . .	16
3.1.2	Upper boundary: Heat flux across a ground surface . .	17
3.2	Presentation of the measurement campaign . . . . .	20

3.3	Model performance assessment . . . . .	23
3.4	Calibration of the materials' properties . . . . .	23
3.5	Methodology of nodes distribution definition . . . . .	25
<b>4</b>	<b>Results</b>	<b>26</b>
4.1	Sensitivity study . . . . .	26
4.1.1	Convective heat transfer coefficient . . . . .	27
4.1.2	Sensitivity of the layer definition . . . . .	29
4.1.3	Deep boundary condition . . . . .	30
4.2	Model ability to reproduce heat conduction transfer: Validation	31
4.3	Influence of the nodes distribution . . . . .	33
<b>5</b>	<b>Discussion</b>	<b>35</b>
5.1	Comparison with other model accuracy . . . . .	35
5.2	Performance according to meteorological data . . . . .	39
<b>6</b>	<b>Conclusion</b>	<b>42</b>

1 **1. Introduction**

2 In global warming circumstances, the development of cities requires to  
3 be carried out considering the urban heat islands (UHI) phenomenon [1] as  
4 a serious environmental issue. This phenomenon has several consequences  
5 on outside comfort and on building energy needs. In order to mitigate the  
6 UHI, it is necessary to identify its causes and to quantify the impact of its  
7 mitigation solutions. Measurements campaigns are useful to evaluate the  
8 UHI but then, linking it to the influence of urban form modifications or  
9 urban planning choices is quite tricky.

10 For that purpose, numerical simulation is a powerful tool. Several mod-  
11 els under development simulate the UHI phenomenon and its consequences.  
12 Different scales are considered depending on the application intended: for  
13 example TEB [2] or ARPS-VUC [3] are more suitable to the city scale ap-  
14 plications while models like SOLENE-microclimat [4], Envi-met [5] and En-  
15 viBatE [6] are dedicated to the district scale. For a same scale, each tool  
16 may have one specific feature among many others : EnviBatE [6] is designed  
17 to study the energy demand of a buildings group, SOLENE-microclimat [4]  
18 focuses on outdoor comfort and on the impact of urban climate on indoor  
19 comfort, and ENVImet [5] is dedicated to outdoor comfort.

20 All those models have in common to represent several physical mecha-  
21 nisms : radiative fluxes, thermal fluxes and fluid dynamic. Furthermore the  
22 representation of those phenomena is essential to calculate precisely the soil  
23 surface temperature, which is the interaction key between the soil and the  
24 urban environment (radiative and sensible fluxes). The heat flux stored and  
25 released by the urban material respectively during day- and night-time is one  
26 of the main causes of UHI development. This heat flux is more important in  
27 urban than in rural areas due to the high inertia of the materials used. Thus  
28 the simulation of heat transfer in the facades but also in the soil are of the  
29 highest importance.

30 The objective of this paper is to propose a model that well reproduces  
31 the heat storage flux into urban ground as well as the surface temperature  
32 evolution.

33 A literature review on models representing heat transfer into soils permits  
34 to identify some lacks as well as to pick up data for the model parametriza-

35 tion.

36 The measurement campaign presented provides input data and validation  
37 data for the model. The chosen indicators to assess the model performance  
38 are then presented. The calibration of the model is carried out and the  
39 different nodes distributions are justified.

40 The results of the study are divided in three parts :

- 41 • sensitivity study on model parameters,
- 42 • model validation using an ideal nodes distribution in order to evaluate  
43 the model ability to reproduce the conductive heat transfer into the  
44 soil,
- 45 • calculation of the accuracy loss caused by different nodes distributions.

46 Then model performances are compared to the ones of models identified  
47 in the literature. Finally the performances are analyzed for a whole year  
48 simulation.

49 This exhaustive study provides accurate information on the reliability of  
50 SOLENE-microclimat, the tool where the soil model is implemented in.

## 51 **2. State of the art**

### 52 *2.1. Existing models*

53 In the literature on microclimate models, the soil representation is rarely  
54 fully described. However, soil models are also used in other fields such as:

- 55 • Geothermal energy applications,

56      • Road applications: pavement sustainability or frost forecasts,

57      • Hydrology and interaction between soil, vegetation and atmosphere.

58 Those other domains have the advantage of proposing a different point of  
59 view on the way to model heat transfer in the ground. In the Table 1 the  
60 articles used for the following bibliographic review are gathered with the  
61 characteristics of the soil models.

Article	Type of application				Surface		Type of coating			Soil column	
	B, GE	Roads	SVA	UM	Previous	Imprevious	Pavement	Bare-soil	Vegetation	Homogeneous	Heterogeneous
Asaeda and Ca (1993, [7])				x	x		x				x
Best (1998, [8])		x			x		x		x	x	
Best and al. (2005, [9])		x			x		x			x	
Bouyer (2009, [4])				x	x		x		x		x
Chow and al. (2011, [10])	x				x				x	irrelevant	
Diefenderfer and al. (2006, [11])		x				x	x			irrelevant	
Gros et al. (2015, [6])				x	x		x				x
Herb et al. (2008, [12])			x		x		x		x		x
Hermansson (2004, [13])		x			x		x				x
Ho (1987, [14])						x	x				x
Jacovides (1996, [15])	x				x		x		x		x
Lin (1980, [16])					x		x				x
Masson (2000, [2])				x			x				
Milhalakou and al. (1997, [17])	x				x				x		x
Milhalakou and al. (2002, [18])	x				x		x		x		
Nowamooz and al. (2015, [19])	x				x		x		x		x
Ozgener and al. (2013, [20])	x				x		x				
Qin and al. (2002, [21])					x		x				x
Saito and Simunek (2009, [22])			x		x		x				x
Swaaid and Hoffman (1989, [23])			x		x						x
Yang and al. (2013, [5])				x	x		x		x		x

Table 1: Models application and type of soil

B, GE: Buildings, geothermal energy SVA: Interaction soil, vegetation, atmosphere UM: Urban Microclimate



62 Even if the field of application is different, all the articles presented have  
63 the common objective of predicting surface temperature, or ground heat  
64 flux. Depending on the application, the physical mechanisms modeled are  
65 not the same. In addition to the conductive heat flux, the moisture flow  
66 is often modeled. This is the case for several applications that use bare-  
67 soil and vegetation covers [21, 22, 12, 7]. This is useful to estimate the  
68 water availability for vegetation or to adjust the thermal properties of the  
69 soil depending on humidity content. Nevertheless, for impervious surfaces,  
70 moisture flux are most of the time neglected [12].

71 The soil model presented in this paper is designed for impervious surface  
72 in urban environment. Urban grounds are heterogeneous and made of differ-  
73 ent layers characterized by large differences regarding their physical proper-  
74 ties. Thus the model shall be able to take into account several layers. In the  
75 literature, the soil is modeled either by an homogeneous or an heterogeneous  
76 column. But for a given area, the size of each layer and its physical properties  
77 are not known accurately. By simplification, half of the soil models presented  
78 here considers an homogeneous column of soil (Table 1). Nevertheless, in or-  
79 der to accurately simulate the conduction flux all along the vertical axis, the  
80 soil profile should be consistent with reality, which implies to consider an  
81 heterogeneous soil.

82 Thermal properties are either set to experimental data (ie : to better  
83 represent measurements albedo is defined as the ratio between incident and  
84 reflected solar radiation) or calibrated.

85 However, the impact of the thermal properties is rarely investigated. Best

86 (1998, [8]) and Herb et al. (2008, [12]) studied the influence of the material  
87 characteristics (diffusivity, specific heat, etc) on surface temperature. Ac-  
88 cording to Best (1998 [8]) and Herb et al. (2008 [12]), the emissivity and  
89 the thermal conductivity of the pavement have the most influence on surface  
90 temperature, while underneath soil characteristics have few influence.

91 In the case of an homogeneous soil column, there are several possibili-  
92 ties to obtain ground temperature variation. Among others, we may cite  
93 the analytical solution (Fourier analysis [9, 10, 14, 15, 17, 18, 20, 23]), the  
94 empirical method [10, 11, 18], or even the Force-restored method [16]. For  
95 an heterogeneous soil column, only the numerical method allows to accu-  
96 rately estimate the surface temperature as well as the ground temperature  
97 for several depths. Twelve of the models described use finite differences  
98 method with an implicit scheme [7, 8, 9, 4, 6, 12, 13, 14, 2, 21, 22, 5] except  
99 Nowamooz et al. (2015, [19]) who use an explicit scheme. The soil model  
100 presented in this paper is based on an implicit finite differences method. The  
101 following section presents in detail all the possible parametrization in the  
102 case of finite differences method.

### 103 *2.2. Parametrization of finite differences models*

104 For a same problem-solving method, different choices can be made re-  
105 garding the nodes distribution (discretization), the boundaries and the initial  
106 conditions (Table 2).

Article	Upper boundary		Convection coeff.		Lower boundary		Initial conditions
	Temperature	Flux	Forced	Natural	Temperature	Flux	
Asaeda and Ca (1993, [7])		x	x		2.5m		EV
Best (1998, [8])		x	x		1.15m		Exponential profile
Best and al. (2005, [9])		x	EV			x	EV
Bouyer (2009, [4])		x	x		2m		Constant value
Gros et al. (2015, [6])		x	CFD		0.5m		NI
Herb et al. (2008, [12])		x	x	x		10m	NI
Hermansson (2004, [13])		x	x	x	5m		NI
Ho (1987, [14])		x		x	x		Linear or exponential profile
Masson (2000, [2])		x	x			x	NI
Nowamooz and al. (2015, [19])	x		irrelevant		4m		EV
Qin and al. (2002, [21])		x	x		x		EV
Saito and Simunek (2009, [22])		x	x		x		EV
Yang and al. (2013, [5])		x	CFD		2m		EV

Table 2: Parametrization of finite differences models

EV: Experimental values NI: No Informations CFD: Computational fluid dynamics

## 107 **Vertical Discretization**

108 Depending on the author, different vertical discretizations are used. Ho  
109 (1987, [14]) and Qin et al (2002, [21]) propose a uniform layout points,  
110 whereas most of the articles present a nodes distribution denser near the  
111 surface than deeper in the ground. Saito and Simunek (2009, [22]) use a  
112 denser distribution near the surface and also near the interface between two  
113 layers. However, the choice of the nodes distribution is rarely clearly jus-  
114 tified. Only Best et al. (2005 [9]) studied the behavior and the accuracy  
115 of the model for different vertical discretization, comparing the numerical  
116 solution with the analytical one. The purpose of the present study is to pro-  
117 pose an optimized discretization which is a compromise between accuracy  
118 loss and computational efficiency. Few sensitivity studies are made on this  
119 point. Asaeda and Ca (1993,[7]) studied the influence of the grid size. As  
120 expected, the thinner the resolution of the grid, the more precise the surface  
121 temperature. This accuracy gain is yet realized to the detriment of calcula-  
122 tion duration. Thus as Best et al. (2005 [9]) suggested, a compromise should  
123 be found between accuracy and execution time.

## 124 **Boundary conditions**

125 To solve one dimension heat conduction equation with the finite differences  
126 method, two boundary conditions are required. The bottom condition taken  
127 at defined depth, can either be a zero flux or a constant temperature (Table  
128 2). If the simulation concerns a short period and the last point of the grid  
129 is below diurnal amortization depth, the type of condition has low influence  
130 on the surface temperature [8].

131 As the purpose of most articles is to predict surface temperature, the  
132 upper boundary condition is defined by the surface energy balance. This  
133 balance is composed of the radiative fluxes, the sensible flux, the latent flux,  
134 and the conductive heat flux in the soil. The long and short wave radia-  
135 tion fluxes are always calculated, except for the validation process for which  
136 measurements are used whenever they are available.

137 As urban soils have a low albedo, temperature gradient between the sur-  
138 face and the air can be very important, especially during clear days. This  
139 phenomenon leads to natural convection (driven by buoyancy forces). In  
140 the surface energy balance, most of the authors only take into account the  
141 forced convective mode (driven by the wind forces), whereas Herb (2008,  
142 [12]) proposes to consider both forced and natural modes.

143 Both Hermansson (2004, [13]) and Herb et al. (2008, [12]) assumed that  
144 the method used to calculate the convective heat transfer coefficient is a crit-  
145 ical point. To test this assumption, they both realized a sensitivity study on  
146 the coefficients of an empirical formula. Herb et al. (2008, [12]) show that  
147 the modification of convection parameters can sometimes have an important  
148 impact on surface temperature : for a 10% increase of the convection param-  
149 eters, the average surface temperature variation is about  $0.24^{\circ}C$ . This might  
150 be explained by low wind speed and by high temperature gradient between  
151 the surface and the air. Hermansson (2004, [13]) dissociates winter and sum-  
152 mer periods, since the temperature gradient between the surface and the air  
153 is smaller during winter. He proposes to use two sets of parameters regarding  
154 solar radiation conditions. Depending on the season, the convection losses

155 and the wind velocity are balanced by coefficients.

### 156 **Initial conditions**

157 In general, few information is given on the initial conditions (temperature  
158 profile) except for the validation process. Most of the authors use exper-  
159 imental values (Table 2). When this information is not available, several  
160 alternatives are proposed : a constant temperature profile is set ([4, 14]) or  
161 an exponential profile between the deep soil and the surface ([8, 14]). How-  
162 ever, according to Ho (1987, [14]), this parameter has low impact on the  
163 surface temperature

## 164 **3. Methodology of the study**

### 165 *3.1. Proposed soil model*

166 The soil model presented in this paper is designed for impervious surface  
167 such as pavement coating. Thus, only heat transfer is taken into account  
168 (moisture transfer is neglected). The soil model is defined as a one dimension  
169 soil column where each layer has its own characteristics. In unsteady state,  
170 the temperature fluctuation is calculated from the Equation 1, which is an  
171 application of the heat equation for a one-dimensional problem.

$$\frac{\delta T}{\delta t} = \alpha_{soil} \cdot \frac{\delta^2 T}{\delta t^2} \quad (1)$$

172  $\alpha_{soil}$  : thermal diffusivity of the soil [ $m^2 s^{-1}$ ]

173 The problem is solved by a finite differences method using a nodal dis-  
174 cretization and an electrical analogy. Heat resistances represent the resis-  
175 tance to heat transfer through a ground layer and heat capacities, the heat  
176 storage capacity of a ground layer. They are defined on Figure 1.

177 The soil model is composed of  $n$  nodes. The energy balance equation is  
 178 calculated at the surface (node  $i = 0$ , Equation 2), and then for each following  
 179 node  $i \in ]0 : n - 1]$  (Equation 3) until the last one which includes the bottom  
 180 boundary condition ( $i = n$ , Equation 4).

$$\frac{T_{surface} - T_{air}}{R_c} + \frac{T_{surface} - T_1}{R_1} + C_e \frac{dT_{surface}}{dt} = R_{net} - LE + H \quad (2)$$

$$\frac{T_i - T_{i-1}}{R_i} + \frac{T_i - T_{i+1}}{R_{i+1}} + C_i \frac{dT_i}{dt} = 0 \quad (3)$$

$$\frac{T_n - T_{n-1}}{R_n - 1} + \frac{T_n - T_\infty}{R_n} + C_i \frac{dT_n}{dt} = 0 \quad (4)$$

183  $R_{net}$ : net radiation [ $W.m^{-2}$ ]

184  $LE$ : latent heat flux [ $W.m^{-2}$ ]

185  $H$ : sensible heat flux [ $W.m^{-2}$ ]

186  $C_e$ : heat capacity of the surface layer [ $J.m^{-2}.K^{-1}$ ]

187  $C_i$ : capacity of the layer at the node  $i$  [ $J.m^{-2}.K^{-1}$ ]

188  $R_c$ : convection resistance [ $m^2.K.W^{-1}$ ]

189  $R_i$ : heat resistance of the layer between the node  $i-1$  and  $i$  [ $m^2.K.W^{-1}$ ]

190  $T_{surface}$ : surface temperature [ $K$ ]

191  $T_{air}$ : air temperature [ $K$ ]

192  $T_i$ : temperature of the node  $i$  [ $K$ ]

193

194 According to this method, any nodes distribution and any boundary con-  
 195 dition depth may be used. Most of the authors in the literature work with  
 196 centimetric grid when accuracy is required. A model with one node per cen-  
 197 timeter is used and defined as the "ideal model" in the following parts. The  
 198 top node is located at the ground surface and the deepest one at a depth of

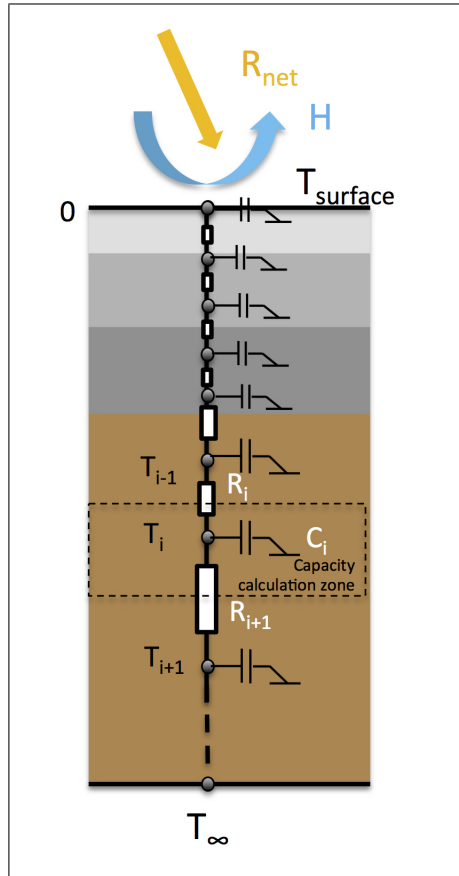


Figure 1: Soil model

199 1m. At this depth, the temperature is supposed to be constant over a day.  
 200 A new value will be set for each day. More details are given in Section 3.1.1.

201 Figure 1 illustrates the way thermal properties are defined. Each layer of  
 202 material is supposed homogeneous and isotropic and has its own character-  
 203 istics which are considered to be constant over time.

204 As the nodes distribution is defined independently from the soil layers and  
 205 characteristics, they are not automatically located at the interface between



206 two layers.

### 207 3.1.1. Deep boundary condition

208 In the deep soil, the temperature is supposed constant over a day. In the  
209 case of an homogeneous soil, an analytic solution can be used to calculate  
210 the temperature for any depth  $z$  and any time  $t$ . If the surface temperature  
211 is considered to be sinusoidal, the analytic solution follows the Equation 5.

$$T(z, t) = T_{ma} + A_a \cdot \exp\left(-\frac{z}{zd_a}\right) \sin\left(w_a(t - t_0) - \frac{z}{zd_a}\right) \quad (5)$$

212  $T_{ma}$ : mean annual temperature [ $^{\circ}C$ ]

213  $A_a$ : annual half amplitude of the climatic thermal wave at the surface [ $^{\circ}C$ ]

214  $zd_a$ : damping depth with an annual beat [ $m$ ]

215  $w_a$ : annual beat  $w_a = 2 * \pi / 31536000$

216  $t_0$ : day of the year where the surface temperature was the coldest

217

218 The parameters  $T_{ma}$ ,  $A_a$  and  $t_0$  are respectively the mean, the amplitude  
219 and the phase of a day surface temperature signal. As a first approximation,  
220 the value for each of those parameters is set according to air temperature sig-  
221 nals. The values used, derived from measurements recorded during 4 years in  
222 three locations of the city of Nantes (FRANCE). The mean annual temper-  
223 ature is  $12.50^{\circ}C$ , the yearly half amplitude of the daily mean temperature  
224 is  $11.86^{\circ}C$  and the phase shift 30 days.

225 From a certain depth, the daily signal is completely damped. The damp-  
226 ing depth depends on the soil characteristics through the parameter  $zd_a$ ,

227 defined by the Equation 6. The depth from where the signal is damped at  
228 95 or 99 % can be estimated from Equation 7.

$$z_{da} = \sqrt{\frac{2 \cdot \alpha_{sol}}{w_a}} \quad (6)$$

229

$$A(z) = A_j \cdot \exp\left(\frac{-z}{z_{da}}\right) \quad (7)$$

230  $A_j$ : half daily amplitude of the climatic thermal wave at the surface [ $^{\circ}C$ ]

231

232 For a range of materials (asphalt, concrete, bare-soil), the most diffusive is  
233 the marble. For this material, the depth corresponding to a daily damping of  
234 99% is 0.89cm. Beyond a meter, the hypothesis is made that the temperature  
235 is constant over the day whatever the type of ground. For this reason, the  
236 bottom node is located below this depth.

### 237 3.1.2. Upper boundary: Heat flux across a ground surface

238 The upper boundary condition is defined from the energy balance at the  
239 ground surface (Equation 8).

$$R_{net} = Q_{cond} + H + LE \quad (8)$$

240 with  $R_{net}$ ,  $Q_{cond}$ ,  $H$ ,  $LE$  previously defined and  $LE=0$  because water fluxes  
241 are not considered in this step of the model.

## 242 Radiative flux

243 The net radiative flux is the balance of all radiative fluxes at the soil  
244 surface. It is the sum of short-wave radiation and long-wave radiation. The

245 historical SOLENE radiative model computes radiative transfers, including  
246 long-wave radiation, inter-reflexion and shading effects [24]. So this input  
247 data doesn't need be calculated in the further model.

## 248 **Convective heat flux**

249 The heat flux exchanged between the surface and a moving fluid can be  
250 expressed with the Equation 9:

$$H = h_c(T_{air} - T_{surface}) \quad (9)$$

251  $h_c$ : convective heat transfer coefficient [ $W.m^{-2}.K^{-1}$ ]

252  $T_{air}$ : air temperature [ $K$ ]

253  $T_{surface}$ : surface temperature [ $K$ ]

254

255 In order to calculate this flux, the convective heat transfer coefficient is  
256 required. In the literature, this coefficient is always a function of wind speed.  
257 Linear or power law functions are used, or correlations using dimensionless  
258 numbers ([25], [26]). For urban applications, the first solution is often used.

259 The most simple is a linear relation of the wind speed (Equation 10). De-  
260 pending on the situation (i.e. surface texture, wind velocity, windward/leeward  
261 surface, etc), Palyvos (2008, [25]) suggests around forty combinations for  $a$   
262 and  $b$  coefficients. For an horizontal surface, with feeble winds ( $V_{air} < 5m/s$ ),  
263 several coefficients are proposed (Table 3).

$$h_c = a + b * V_{air} \quad (10)$$

264  $V_{air}$ : wind speed [ $m.s^{-1}$ ]

265

<b>Reference</b>	<b>a</b>	<b>b</b>
McAdams (1954, [27])	5.7	3.8
ASHRAE (1993)	5.62	3.9
Cristofari et al. (2006)	5.67	3.86

Table 3: Coefficients  $a$  and  $b$  for a flat surface low wind speed

266 Methods based on correlations that use dimensionless numbers (Reynolds,  
267 Grashof, and Nusselt) also exist. For flat surfaces Morille (2012, [28]) presents  
268 coefficients depending on the flow regime (Table 4).

<b>Convection mode</b>	<b>Flow regime</b>	$a$	$b$	$c$	$d$	$e$
Free	laminar	0	0	0.49	1/4	1
	turbulent	0	0	0.13	1/3	1
Mixed	laminar	1	3/2	0,57	3/5	0,68
	turbulent	1	12/5	12,1	1/3	0,03
Forced	laminar	0,56	1/2	0	0	1
	turbulent	0,03	4/5	0	0	1

Table 4: Coefficients in function of the convection mode for a flat surface

$$h_c = e(aRe^b + cGr^d) \quad (11)$$

269

$$Nu = \frac{h_c \cdot L_c}{\lambda_{fluid}} \quad (12)$$

270  $Re$ : Reynolds number

271  $Gr$ : Grashof number

272  $Nu$ : Nusselt number

273  $L_c$  : characteristic length [ $m$ ]

274  $\lambda_{fluid}$ : thermal conductivity of the fluid [ $W.m^{-1}.K$ ]

275

276 This type of correlation allows to define a convective heat transfer coef-  
277 ficient as a function of the flow modes:

- 278 • Natural or free convection: air flow driven by buoyancy forces,
- 279 • Forced convection: air flow driven by wind forces,
- 280 • Mixed convection: when the air flow is created by both wind and buoy-  
281 ancy forces.

282 In the case of urban applications, wind speed is often feeble and the  
283 temperature gradient important. Then free convection may become predom-  
284 inant. A comparison between the MacAdams formula and the correlation  
285 method is performed in order to choose the most suitable method for urban  
286 climate application (Section 4.1.1).

### 287 *3.2. Presentation of the measurement campaign*

288 The measurement campaign provided data that are used either as model  
289 inputs or as validation data to evaluate the model performance and its accu-  
290 racy.

291 Data from the ROSURE/HydroVille project are used. This project was  
292 leaded by IFSTTAR and funded by the National Institute for Earth sciences  
293 and Astronomy (INSU) of the *Centre National de la recherche scientifique*

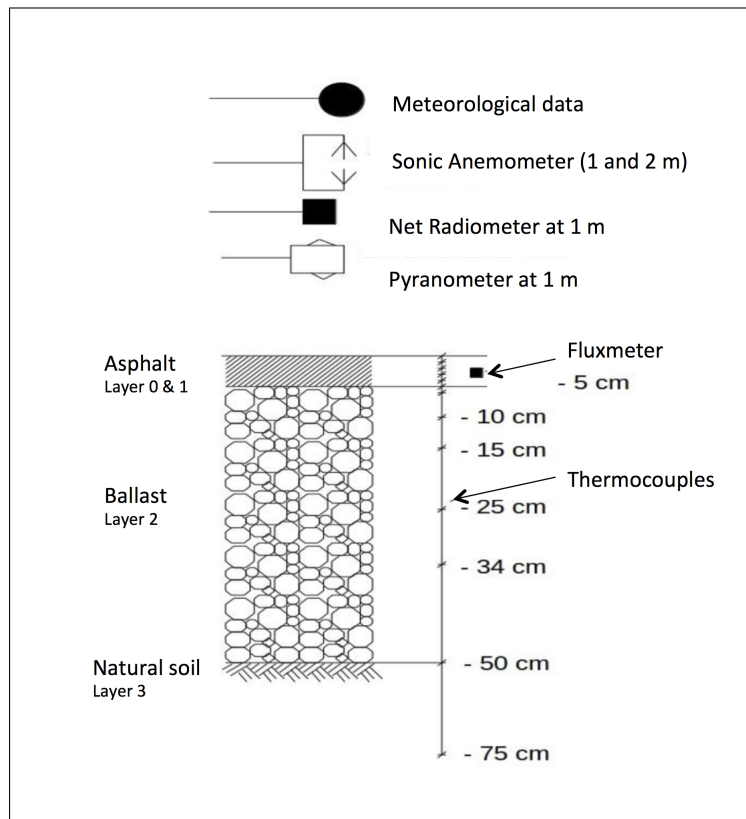


Figure 2: Drawing of the measurement campaign

294 (CNRS). A campaign devoted to the documentation of energy and water  
 295 budgets of an asphalt parking lot was carried out in the month of June,  
 296 2004. This campaign especially focused on surface and air temperatures and  
 297 on heat flux measurements during a warm summer period. Artificial rain  
 298 events were performed during the campaign but the present study only focus  
 299 on dry weather periods.

300 The experiment site is located near Nantes (France) within the IFSTTAR  
 301 center of Bouguenais, and consisted in an asphalt parking lot of 2500 square  
 302 meters. The soil structure is composed of a 5cm- asphalt layer, a 45cm-

303 ballast layer and natural soil underneath. Along the observations available  
304 for this campaign, this study focused on the following variables, all observed  
305 in the middle of the parking lot (Figure 2):

- 306 • surface and ground temperatures; a vertical profile was placed with  
307 type T thermocouples (diameter  $120\mu m$ ) located at 0, 1, 2, 3, 4, 5, 6,  
308 10, 15, 24, 34, 50 and 75 cm depth.
- 309 • wind speed and direction (Young Campbell (05103) monitor);
- 310 • humidity and air temperature at 1 and 2m above ground; HMP45C  
311 TRH probes (Campbell) with Vaisala HR HUMICAP for humidity and  
312 PT1000 for temperature.
- 313 • convective heat fluxes at 1 and 2m height; sonic anemometer USA1  
314 (Metek)
- 315 • radiation components, thanks to 4 pyranometers and a radiometer at a  
316 height of 1m; 2 pyranometers CM6B (Kipp & Zonen), 2 pyranometers  
317 CGR3 (Kipp & Zonen) and a net radiometer NRLite (Kipp & Zonen).

318 The data were collected with a 1 min time step except for the sonic  
319 anemometer (0,1 s). The final data are averaged to 15 min time steps. From  
320 the whole measurement period, two consecutive days are selected with dif-  
321 ferent meteorological conditions: one cloudy sky day ( 5<sup>th</sup> of june) and one  
322 clear sky day ( 6<sup>th</sup> of june). The clear sky day will be used to calibrate the  
323 model while the cloudy day will be used to evaluate the model.

324 *3.3. Model performance assessment*

325 Several indicators may be used to evaluate the performance of a soil  
326 model. Most of the authors focus on the ability of their model to estimate  
327 surface temperature. Only few of them go further in the analysis evaluating  
328 the heat flux calculation or the ground temperature at different depths.

329 In this article, the indicator chosen is the RMSE (Root Mean Square  
330 Error). As most of the authors used it, it will be easier to compare the  
331 model accuracy. In order to evaluate if the dynamic of heat storage is well  
332 reproduced, the RMSE will be calculated at the surface and at several depths.

333 *3.4. Calibration of the materials' properties*

334 As seen before, the thermal characteristics of the soil are often unknown  
335 and must be adjusted to well represent fluxes and temperatures variations.  
336 The characteristics of the soil layers are calibrated according to the observed  
337 soil profile, reducing the difference between the measured and simulated sur-  
338 face temperature. Data acquired on the 6<sup>th</sup> of June are used for calibration.

339 Temperature gradient is initialized from ground temperatures measured  
340 on 5<sup>th</sup> of June at midnight. The deep boundary condition, corresponding  
341 to the ground temperature at 75 cm depth is set according to experimental  
342 data.

343 Albedo and emissivity of the surface are calculated from short and long  
344 wave radiations measured during the period of interest. For the albedo, the  
345 mean diurnal value is 0.173 (for reflected short-wave radiation flux  $K_{up} >$   
346  $20W/m^2$ ), and the mean emissivity value over the period is 0.965.



347 The thermal characteristics (Figure 2) are adjusted by an iterative pro-  
 348 cedure reducing the difference between the measured and simulated temper-  
 349 ature at the surface and various depths. The thermal characteristics values  
 350 are considered acceptable when the RMSE on each ground temperature has  
 351 the same level of magnitude than the uncertainty of the sensor ( $0.3K$ ).

352 Yang et al. (2013, [5]) noticed that thermal characteristics of the asphalt  
 353 layer may vary with depth. Due to the asphalt compaction, the layer density  
 354 and the asphalt proportion are not constant along depth, altering the thermal  
 355 properties. Yang et al. (2013, [5]) made the choice to divide the asphalt  
 356 layer into several layers to which different properties were attributed. The  
 357 same phenomena is observed through the analyze of the temperature signal  
 358 within the asphalt layer. For this reason, the asphalt layer is divided in two  
 359 layers (respectively one of 1cm, and one of 4cm). The calibrated material  
 360 characteristics are summarized in the Table 5.

<b>Layer</b>	<b>Depth</b>	<b>Thermal conductivity</b>	<b>Volumetric heat capacity</b>
Number	m	$W/(m.K)$	$J/(m^3.K)$
0	0.01	2.5	2.3
1	0.05	2.5	2.1
2	0.5	1.8	2.3
3	1	1.3	2.1

Table 5: Calibrated characteristics of the soil

361 *3.5. Methodology of nodes distribution definition*

362 Optimization of the nodes distribution is one of the major modeling chal-  
 363 lenge. The principle consists in reducing the number of nodes up to a situa-  
 364 tion where calculation time and lack of accuracy are minimal.

<b>Zone</b>	<b>Depth of the part [m]</b>	<b>Criterion</b>
1	0.08	Amortization depth for the material with the highest diffusivity and three hourly pulsation
2	0.4	Amortization at 95% of the daily signal for the most common material for this part ( soil, concrete, stone)
3	1.0	Amortization at 95% of the daily signal for the material with the highest diffusivity

Table 6: Criterion for the choice of each zone's size

365 For the grid optimization, the choice was made to work with annual  
 366 simulation. First, an analytic solution is used to better understand ground  
 367 temperature dynamic. In this way, two sinusoidal temperature signals are  
 368 applied to the surface: a three hours period (corresponding to weather change  
 369 or shadow created by building during a day) and a day period (corresponding  
 370 to the day-night cycle). Closer we get to the deep condition, more linear  
 371 the profile. With finite differences method, more linear is the profile, less  
 372 dense the distribution of node needs to be. According to this result, nodes  
 373 distribution is different in the three zones : the criteria used to identify each  
 374 of them are given in Table 6.

375 Then, three nodes distributions are proposed to better represent those  
 376 ground temperature profiles (Figure 3). The final distribution profiles are  
 377 consistent with those proposed in the literature: the nodes density is higher  
 378 in the upper layer of the ground than in the lower layers.

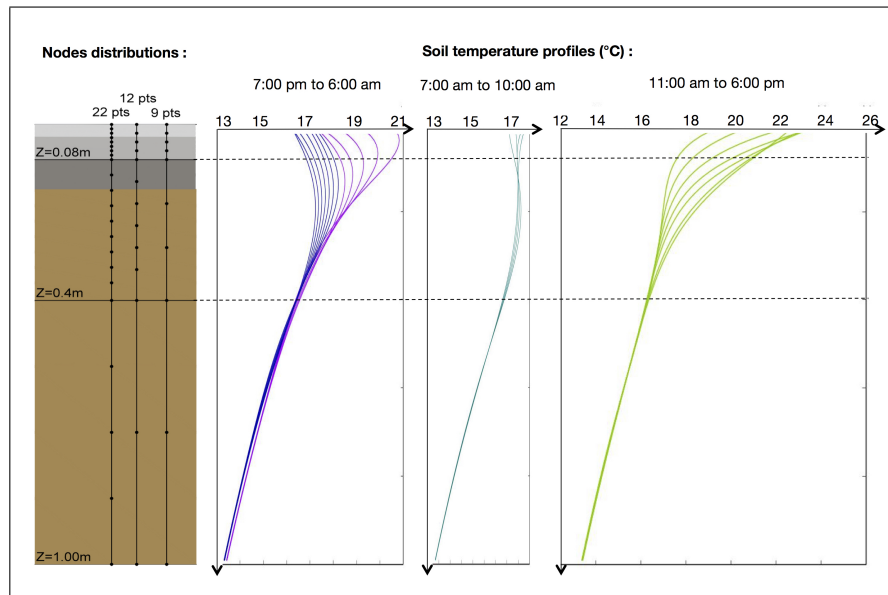


Figure 3: 3 nodes distributions proposal

## 379 4. Results

### 380 4.1. Sensitivity study

381 Some assumptions made for the model parametrization can affect the sur-  
 382 face temperature calculation. Some authors realized a sensitivity study on  
 383 the surface and material parameters, on the convective heat transfer coeffi-  
 384 cient or on the grid size. However, none of those studies has compared the  
 385 relative influence of all the affecting parameters. In the following section, a

386 model sensitivity study is performed on the surface temperature. Two kinds  
387 of parameters are used for this study : those used for the calibration step (soil  
388 thermal characteristics and the convective heat transfer coefficient) and two  
389 additional parameters which have been identified to be relevant: the deep  
390 boundary conditions and the size of the layers. The parameters sensitivity is  
391 studied regarding the order of magnitude of its uncertainty.

#### 392 *4.1.1. Convective heat transfer coefficient*

393 Several methods are presented to estimate the convective heat transfer  
394 coefficient  $h$  in Section 3.1.2. Two methods are first compared to select the  
395 most suitable one:

- 396 • MacAdams (1954, [27]) formula: linear function of the wind speed  
397 (coefficients  $a$  and  $b$  respectively equal to 3.8 and 5.7).
- 398 • Correlation equation with dimensionless numbers and different charac-  
399 teristics length (1, 10, 50 m).

400 The Figure 4 illustrates the comparison. For the correlation method, after  
401 calculation of the dimensionless coefficients, the convection mode varies over  
402 time: it is mostly mixed during the night and forced during the day. The  
403 free convection is not represented with the first formula whereas it is not  
404 integrated in the MacAdams formula. The correlation method is closer to  
405 the measured heat flux all over the comparison period.

406 The correlation method used to calculate the convective heat transfer co-  
407 efficient (Section 3.1.2), is based on results obtained by Tain and Petit (1989,

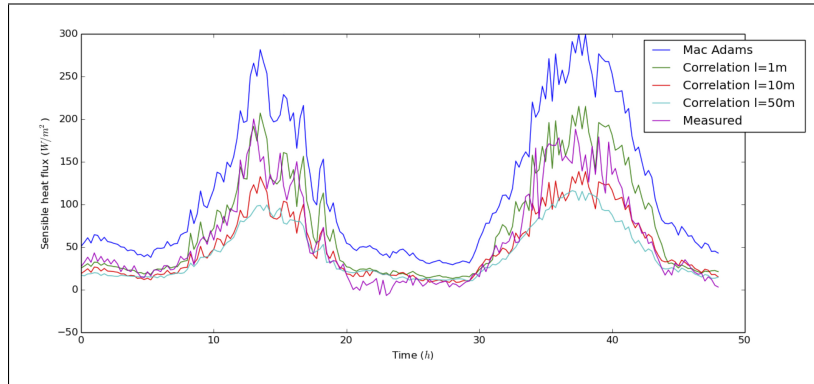


Figure 4: Comparison of sensible heat fluxes (*print in color*)

408 [29]) applied for an horizontal flat plate. In order to apply the similitude theory,  
 409 a characteristic length should be set which is most of the time defined  
 410 as the distance from the leading edge. Applied to our case, this characteristic  
 411 length is difficult to define. The influence of several lengths (1, 10 and  
 412 50 m) is tested (Figure 4). Among the tree values tested, it appears that  
 413 the 1m- characteristic length correlation method produces the lowest RMSE  
 414 ( $24.27W/m^2$ ).

415 For each value, the correlation method remains better than the MacAdams  
 416 method. As a result, for the following sub-sections, the correlation method  
 417 is chosen with a characteristic length of 1m.

418 In order to see the influence of the characteristic length value on the  
 419 sensible heat flux, the RMSE calculated with the 1m- characteristic length  
 420 is compared to the daily mean sensible heat flux ( $61W/m^2$ ). The RMSE  
 421 represents 40% of the mean experimental value.

422 According to those levels of magnitude, we realize the sensitivity study

423 varying the convective heat transfer coefficient up to 40% of its initial value.  
 424 The aim is here to quantify the influence of this coefficient on the surface  
 temperature. The results are presented on the Table 7.

<b>Indicator</b>	$h + 40\%$	$h - 40\%$
Maximum error ( $^{\circ}C$ )	3.70	5.46
Mean error ( $^{\circ}C$ )	1.89	2.78
RMSE ( $^{\circ}C$ )	2.12	3.14

Table 7: Influence of the convective heat transfer coefficient on the surface temperature (5<sup>th</sup> and 6<sup>th</sup> of june)

425

#### 426 4.1.2. Sensitivity of the layer definition

427 Modification of soil thermal conductivity, soil density and the thickness  
 428 of the layers is performed one by one for each layer. The magnitude of the  
 429 modifications and the layers concerned by the modification are described in  
 430 the Table 8. The surface temperature modification caused by each material  
 431 property change is also presented in this Table.

432 The height of each soil layer is not constant over the depth. Each height  
 433 is then roughly estimated. To evaluate this lack of accuracy, the influence of  
 434 the biggest layers (1 and 2) is investigated (Table 8).

435 The temperature change associated to layer size modification has the  
 436 same magnitude as the one associated to soil property modification of the  
 437 layers 0 and 3. However, it is negligible compared to temperature change  
 438 associated to soil property modification of the layers 1 and 2.

Parameter	Modified layer	Maximum difference at the surface ( $^{\circ}C$ )
Thermal conductivity	0	$< 0,1$
$\lambda + -10\%$	1	$< 0,7$
	2	$< 0,7$
	3	$< 0,1$
Density	0	$< 0,07$
$\rho + -5\%$	1	$< 0,3$
	2	$< 0,3$
	3	$< 0,07$
Size of the layer	1	$< 0,04$
$e + -0,01m$	2	$< 0,15$

Table 8: Influence of the soil characteristics ( $5^{th}$  and  $6^{th}$  of june)

439 *4.1.3. Deep boundary condition*

440 The temperature imposed as deep boundary condition can have an influ-  
441 ence on the surface temperature. If the deep temperature is overestimated  
442 by one degree, the difference on surface temperature is only of  $0.05^{\circ}C$ .

443 Finally, the convective heat transfer coefficient is the most influent pa-  
444 rameter , followed by the material characteristics, the layer size and the deep  
445 boundary condition.

446 4.2. Model ability to reproduce heat conduction transfer: Validation

447 The ability of the model to well reproduce the physical phenomenon is  
448 evaluated in this part. In order to quantify the uncertainty due to the model  
449 itself (i.e. the accuracy of the physical phenomenon representation), the  
450 model is first evaluated comparing temperature estimation to experimental  
451 data. As it was noticed in Section 3.3, the evaluation of a soil model per-  
452 formance only based on surface temperature comparison is one of the lack  
453 identified in the literature. In this study, the comparison of the results is  
454 realized on the basis of the temperature at the surface and at several depths  
455 in the soil.

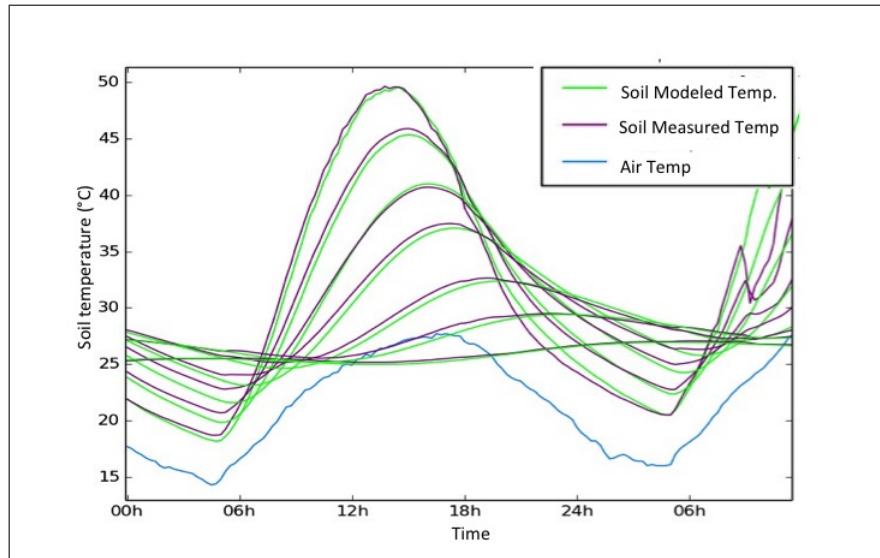


Figure 5: Comparison of simulated and measured temperatures at the surface and at several depths (*print in color*)

456 The model is evaluated during the 5<sup>th</sup> and the 6<sup>th</sup> of June. The model  
457 reproduces correctly the heat flux conducted into the different layers of the



458 soil as shown in the Figure 5. The maximum difference between the measured  
 459 and simulated temperature at the surface is  $1.91^{\circ}C$  and the RMSE  $0.75^{\circ}C$ .

460 To quantify the accuracy of the model to reproduce the temperature vari-  
 461 ation at several depths, Qin (2002, [21]) divide the RMSE per the amplitude  
 462 of the signal. In fact as the amplitude decreases, the relative error increased.  
 463 To avoid this bias, the standard deviation of the experimental data is used  
 464 instead of the amplitude. This is a more robust indicator against outliers  
 465 (Table 9). Going deeper in the ground the amplitude decreased with the  
 466 RMSE but in proportion this error is increasing. In fact, at the surface, the  
 467 RMSE only represents 8% of the signal standard deviation when at a depth  
 468 of 34 cm and 50cm it represents respectively 16% and 12%. The error stays  
 469 under the uncertainty of the temperature measurement.

<b>Depth</b>	<b>Maximum absolute error (<math>^{\circ}C</math>)</b>	<b>RMSE (<math>^{\circ}C</math>)</b>	<b>RMSE/standard deviation</b>
Surface	1.61	0.75	0.08
5 cm	1.42	0.73	0.09
10 cm	0.83	0.48	0.09
34 cm	0.52	0.21	0.16
50 cm	0.13	0.06	0.12

Table 9: Evaluation of the ideal model according to the experimental data (5<sup>th</sup> and 6<sup>th</sup> of june)

470 *4.3. Influence of the nodes distribution*

471 The ability of the model to reproduce the physical phenomenon (ideal  
 472 model compared to the experimental data) is compared to the accuracy loss  
 473 due to the reduction of the number of nodes. Table 10 presents the total  
 474 error due to the model and the nodes distribution (first line) and the part of  
 475 the error which is due to the nodes reduction (2nd line).

<b>Model</b>	<b>1pt/cm</b>	<b>8/10/4</b>	<b>4/6/2</b>	<b>4/3/2</b>
Root mean square error with ex- perimental data ( $^{\circ}C$ )	0.75	1.12	1.23	1.56
Root mean square error with ideal model ( $^{\circ}C$ )	-	0.28	0.75	1.36

Table 10: Evaluation of the model with reduced numbers of points ( $5^{th}$  and  $6^{th}$  of june)

476 For the 8/10/4 points model, the reduction of the number of points has a  
 477 negligible influence compared to the uncertainty of the temperature measure-  
 478 ment. Even if the total error of this model with experimental data ( $1.12^{\circ}C$ )  
 479 increases, this justifies that a higher number of points could not be so rele-  
 480 vant since the uncertainty do not permits to say if the model precision would  
 481 be higher or not. In all cases, number of nodes is not the main cause of the  
 482 error.

483 For the 4/6/2 points model, the RMSE is the same if the model is com-  
 484 pared with the experimental data or with the ideal model. This means that  
 485 the reduction of the model remains acceptable.

486 Finally for the 4/3/2 model, the accuracy loss due to the reduction of the  
487 number of nodes becomes dominant.

488 For all models, non-cumulative errors are observed. For instance, the  
489 4/3/2 model accuracy ( $1.56^{\circ}\text{C}$ ) remains lower than the loss of accuracy due  
490 to the node number reduction ( $1.36^{\circ}\text{C}$ ) added to the error between measure-  
491 ments and the ideal model ( $0.75^{\circ}\text{C}$ ).

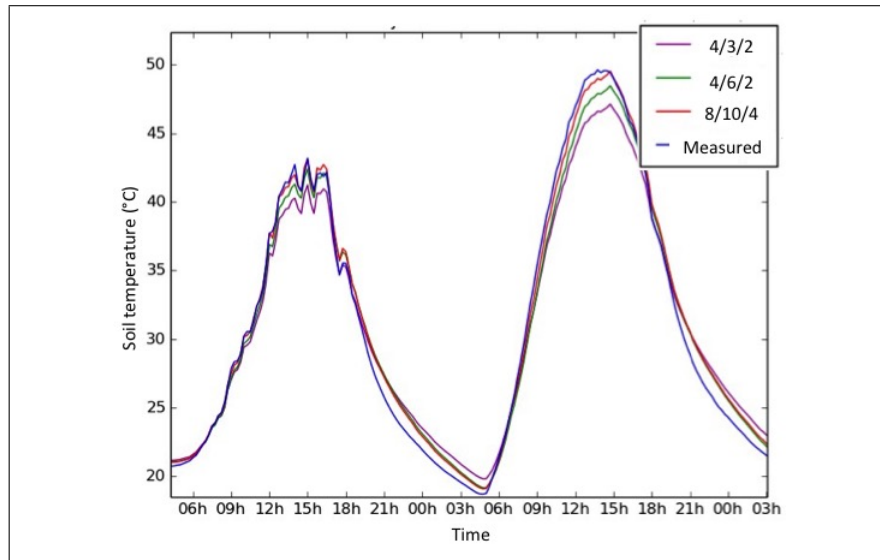


Figure 6: Surface temperature calculated with the different numbers of nodes compared to measured one. (*print in color*)

492 Figure 6 compares the surface temperature evolution of the different mod-  
493 els with the measured one. Firstly, all the models represent well the time  
494 evolution of the surface temperature. Nevertheless, the daily maximum and  
495 minimum peak are underestimated. This is due to the nodes number re-  
496 duction that leads to worsen the representation of the heat transfer into the

497 floor. In fact, this induces a time shift of the heat conduction whose the main  
498 influence of which appears when its sign changes.

499 Finally, the lower number of points for the model, the higher the under-  
500 estimation of the daily maximum and minimum peak. Indeed the reduction  
501 of the number of points has consequences on the reproduction of the daily  
502 peaks. As a conclusion, this confirms that the correct representation of the  
503 surface temperature requires to correctly represent heat flux transfer into the  
504 soil.

## 505 **5. Discussion**

506 This part is devoted to discuss the overall accuracy of the model. The  
507 results are firstly compared to those presented in the literature. Then the  
508 accuracy of the model according to meteorological data is evaluated with an  
509 annual simulation.

### 510 *5.1. Comparison with other model accuracy*

511 The performance of the models presented above may be compared to the  
512 performance of others models. Among literature the results of the following  
513 authors are chosen: Yang et al. (2013 [5]), Herb et al. (2008 [12]), Best  
514 (1998 [8]) , Malys, (2012 [30, 24]). Note that Malys, (2015, [30, 24]) applied  
515 the model proposed by Bouyer (2009, [4]). Those models are chosen because  
516 their simulation conditions (weather conditions, nodal distribution, type of  
517 ground surface, indicator calculated for performance evaluation) are the clos-  
518 est to those of the present study. Conditions of simulation and results are  
519 summarized in Table 11.

520 Three of the four articles ([5, 8, 12]) have in common the type of surface  
521 studied and a gradual distribution of nodes: thinner at the surface than  
522 bellow. The last one, Malys (2012, [30, 24]) evaluated SOLENE-microclimat  
523 previous soil model with a grass surface and a nodal distribution of only 4  
524 nodes.

525 Simulations are run during summer period for clear and hot days. Indeed  
526 the surface temperature rise from  $41^{\circ}C$  to  $70^{\circ}C$ , except for Best (1998, [8]),  
527 who worked with lower temperature.

528 According to the results presented in Table 11, the ideal model is more  
529 accurate than the four other models from the literature. This is a logical  
530 result as this ideal model use an high number of nodes.

531 Best model (1998, [8]) accuracy ( $1.2^{\circ}C$ ) is similar to the 8/10/4 points  
532 model. Nevertheless, as it is applied for winter conditions, the solicitations  
533 are softer (amplitude of  $18^{\circ}C$  ) than the ones of this study.

534 Using a 15 nodes model, Herb et al. (2008 [12]) obtained lower perfor-  
535 mances ( $1.58^{\circ}C$ ) than the 8/10/4 points model ( $1.12^{\circ}C$ ) and the 4/6/2 points  
536 model ( $1.23^{\circ}C$ ) but similar performances than the 4/3/2 model ( $1.56^{\circ}C$ ).  
537 The application conditions being similar, it can be affirmed that our model  
538 is at least as accurate model as Herb et al. (2008 [12]) model but with a  
539 more optimized discretization. The difference of performance can mainly be  
540 explained by a thinner discretization near the surface.

Article	Surface type	Meteorological conditions	Maximum surface temperature C	Amplitude	Numerical discretization	RMSE °C
Best (1998, [8])	Asphalt	Winter conditions	-	-	20 nodes	1.08
	Concrete		12	18		1.2
Herb and al. (2008, [12])	Asphalt	Hot and Dry (July)	55	30	15 nodes	1.58
Malys (2012, [30])	Grass	Hot and Dry (May)	41	19	4 nodes	2.3
	Tiles, concrete,					
Yang and al. (2013, [5])	asphalt, paved,	Hot and Dry (August)	70	40	14 nodes	1.98
	grass					
Presented here	Asphalt	Heat wave conditions	50	30	100 nodes	0.75
					8/10/4	1.12
					4/6/2	1.23
					4/3/2	1.56

Table 11: Comparison with the other models: simulation conditions

541 Yang et al. (2013, [5]) presented a 14 layers model with  $1.98^{\circ}C$  accuracy  
542 which is lower than all the models evaluated in this paper. Nevertheless, it  
543 is applied to extremes conditions : maximum surface temperature can reach  
544  $70^{\circ}C$  with a daily variation whose amplitude reaches  $40^{\circ}C$ .

545 Our 8/10/4 points model has the same accuracy than Best model (1998,  
546 [8]) but under disadvantageous conditions : surface temperature amplitude  
547 is much higher in the present study ( $31^{\circ}C$ ) than the one used by Best (1998,  
548 [8]) ( $18^{\circ}C$ ). For similar surface temperature amplitude (respectively  $< 30^{\circ}C$   
549 and  $40^{\circ}C$ ), Herb et al. (2008 [12]) and Yang et al. (2013, [5]) obtained a  
550 RMSE of  $1.58^{\circ}C$  and  $1.98^{\circ}C$ .

551 The model presented by Malys (2012, [30]) has only four nodes whereas  
552 the other models have more than 14 nodes. Consequently, it is the least ac-  
553 curate one even if the model is applied with fair solicitations : low amplitude  
554 of the surface temperature variation ( $19^{\circ}C$ ) and low maximum temperature  
555 ( $41^{\circ}C$ ) . Using a higher number of nodes with good distribution seems to  
556 be essential to obtain good performances. However, caution should be taken  
557 with this result since Malys (2012, [30]) does not use the same ground surface  
558 type than the other authors.

559 Two of the authors highlight that the high amplitude of surface tem-  
560 perature recorded during the day is harder to represent than the surface  
561 temperature during the night. Yang et al.(2013, [5]) described the fact that  
562 the model fits well with the measurement at night time and in the morning,  
563 but when the temperature rises during the afternoon, the model underesti-  
564 mates the temperature with an average of  $3.5^{\circ}C$ . Best (1998, [8]) also has

565 best results during the night (RMSE  $0.83^{\circ}C$  ) than during the day (RMSE  
566  $1.26^{\circ}C$ ). This analysis is consistent with the assumption made previously:  
567 clear and hot days, characterized by high surface temperature amplitude, are  
568 the most difficult days to simulate.

569 In general, one needs to be careful considering the results of this compar-  
570 ison for several other reasons :

- 571 • surface temperature used as the reference temperature for each study  
572 comes from surface temperature measurement. Uncertainty on such  
573 measurement might be the same magnitude than the RMSE observed,  
574 which makes comparison between models difficult.
- 575 • The comparison of the models performance is given for study in similar  
576 conditions. Nevertheless they cannot be exactly the same. Localization  
577 is not the same, weather conditions differ, surface type or at least soil  
578 composition is not exactly the same.

579 If we concluded that the models proposed in this paper seem to present a  
580 better performance than those of the literature, the difference must be put  
581 into perspective with application conditions. All those models should be  
582 applied to a single case study.

### 583 *5.2. Performance according to meteorological data*

584 The accuracy of a nodes distribution according to meteorological data  
585 is evaluated comparing numerical profile of an annual simulation (hourly  
586 time step) for each nodes distribution (8/10/4, 4/6/2, 4/3/2). For those



587 simulations, meteorological data recorded during one year (2010) at the Pin  
 588 Sec station of the city of Nantes are used. Those data were collected by the  
 589 ONEVU (Observatoire Nantais des EnVironnements Urbains) : observatory  
 590 of the urban environment of the IRSTV (Mestayer et al. 2011 [31]). Among  
 591 the available observations, the following data are used as input in the model:  
 592 air temperature, pressure and humidity; global and IR radiative flux; wind  
 593 velocity and direction.

	<b>8/10/4</b>	<b>4/6/2</b>	<b>4/3/2</b>
Part 1	1pt/cm	1pt/2cm	1pt/2cm
Part 2	1pt/3.5cm	1pt/5cm	1pt/10cm
Part 3	1pt/15cm	1pt/30cm	1pt/30cm
Total number of points	22	12	9
Maximum absolute difference with the ideal model over a year ( $^{\circ}C$ )	0,58	1,35	2,18
Yearly mean absolute difference with the ideal model ( $^{\circ}C$ )	0,1	0,2	0,33

Table 12: Distribution of the points and precision

594 Table 12 presents the results of the comparison between the surface tem-  
 595 perature model for each of the nodes distribution compared to the ideal

596 model. In the case of the 8/10/4 points model, the maximum absolute dif-  
 597 ference is  $0.58^{\circ}C$  and for the 4/3/2 points model  $2.18^{\circ}C$ . The mean absolute  
 598 difference for the first node distribution is only  $0.1^{\circ}C$  whereas the one of the  
 599 4/3/2 distribution is  $0.33^{\circ}C$ , which remains in the order of magnitude of the  
 600 measurement uncertainty.

601 For each case, the appearing frequency of the mean daily error between  
 602 the ideal and the reduced model is calculated. Every day is classified in a  
 603 different class of performance to illustrate the differences between the nodes  
 604 distributions (Table 13).

<b>Mean daily error</b>	<b>Low : <math>E &lt; 0.2</math></b>	<b>Medium: <math>0.2 &lt; E &lt; 0.5</math></b>	<b>High <math>E &gt; 0.5</math></b>
8/10/4	363	2	0
4/6/2	212	150	3
4/3/2	82	224	59

Table 13: Number of days for which each class of error occurs.(error calculated compared the ideal model)

605 The 8/10/4 points model does not have any day having a mean error  
 606 higher than  $0.5^{\circ}C$  and has only two days with a mean error higher than  
 607  $0.2^{\circ}C$ . The 4/6/2 points model has almost as many days represented with a  
 608 high or a medium performance. Finally most of the days represented by the  
 609 4/3/2 points model have medium performance. More detailed investigation  
 610 of the days with high mean daily error shows that these days were clear  
 611 and sunny ones. This confirms the fact that clear day are more difficult to  
 612 simulate than cloudy days.

## 613 **6. Conclusion**

614 The main purpose of this study is to propose a model that well repro-  
615 duces the heat storage flux into urban ground as well as surface temperature  
616 evolution.

617 Some lacks were identified in the literature review pointing up the need:

- 618 • to perform overall sensitivity analysis,
- 619 • to investigate the interest of using different convection flow modes  
620 (forced, mixed, natural)
- 621 • to justify the choice of nodal distribution,
- 622 • to assess models not only for surface temperature calculation.

623 To test the robustness of our model regarding its parameters, a complete  
624 sensitivity study was achieved on the model parameters: all have a negligible  
625 impact except the convective heat transfer coefficient.

626 Special attention has been paid to the way to calculate the convective  
627 heat transfer coefficient. The chosen method permits to take into account  
628 the different kind of convection flow modes which is necessary for urban  
629 application. Nevertheless, the sensible heat flux can vary of 40%, leading to  
630 an uncertainty up to  $3.14^{\circ}C$  on the surface temperature RMSE.

631 After the calibration of the different parameters, the soil model (using an  
632 "ideal" node distribution - 1 node/cm) accuracy is evaluated according to a  
633 measurement campaign that is realized on a large asphalt parking lot during

634 two clear and sunny days. The RMSE between estimated and observed  
635 temperature is calculated for surface temperature and ground temperature at  
636 several depths. Surface temperature RMSE is  $0.75^{\circ}C$ , RMSE for temperature  
637 at 34cm of depth is  $0.21^{\circ}C$ . The results validate the ability of the model to  
638 well reproduce the heat storage into the ground.

639 Three nodes distributions are proposed on the base of the analyze of the  
640 different temperature profiles along the depth. They all are dedicated to  
641 any kind of urban impervious surfaces. However, for less diffusive soils, the  
642 user is free to define other distributions in order to adapt the model to his  
643 application. The accuracy of the models varies from  $1.12^{\circ}C$  to  $1.56^{\circ}C$ . These  
644 performances are better than those of models from the literature applied  
645 under quite similar conditions.

646 Finally, the application of the models all over a year shows that only few  
647 days are represented with an accuracy worse than  $0.5^{\circ}C$ . Most of the days  
648 are even reproduced with an accuracy better than  $0.2^{\circ}C$ . The investigation  
649 demonstrates that the surface temperature during clear and sunny days are  
650 the most difficult to reproduce.

651 This paper provides a complete overview of a soil model performance,  
652 comparing it with experimental data, ideal model and literature results. Be-  
653 cause of the measurement uncertainty, better performances would be difficult  
654 to obtain and especially to assess. Nevertheless, the comparison of the model  
655 performances with results from literature would require a benchmark. The  
656 presented model, now validated is now ready to include the moisture trans-  
657 fers and in particular the evaporation of water at the soil surface so that to

658 help to assess properly the effect on local climate and outdoor comfort of  
659 moistening techniques.

## 660 **Acknowledgements**

661 This research work was carried out within the scope of the EVA Project,  
662 funded by the ADEME (French Environment and Energy Management Agency)  
663 under Contract No. 1216C0037. The authors are grateful to the ADEME and  
664 Véolia for their financial support of this study, as well as to the IFSTTAR,  
665 the LHEEA and the ONEVU for providing us the experimental data.

- 666 [1] T. R. Oke, *Boundary layer climates*, Routledge, 2002.
- 667 [2] V. Masson, A physically-based scheme for the urban energy budget in  
668 atmospheric models, *Boundary-layer meteorology* 94 (2000) 357–397.
- 669 [3] R. Tavares, I. Calmet, S. Dupont, Modelling the impact of green infras-  
670 tructures on local microclimate within an idealized homogeneous urban  
671 canopy, in: *ICUC9-9th International Conference on Urban Climate*  
672 *jointly with 12th Symposium on the Urban Environment Modelling*, pp.  
673 1–6.
- 674 [4] J. Bouyer, *Modelisation et simulation des microclimats urbains-Etude de*  
675 *l’impact de l’aménagement urbain sur les consommations energetiques*  
676 *des batiments*, Ph.D. thesis, Universite de Nantes, 2009.
- 677 [5] X. Yang, L. Zhao, M. Bruse, Q. Meng, Evaluation of a microclimate  
678 model for predicting the thermal behavior of different ground surfaces,  
679 *Building and Environment* 60 (2013) 93–104.

- 680 [6] A. Gros, Modélisation de la demande énergétique des bâtiments à  
681 l'échelle d'un quartier, Ph.D. thesis, Université de La Rochelle, 2013.
- 682 [7] T. Asaeda, V. T. Ca, The subsurface transport of heat and moisture  
683 and its effect on the environment: a numerical model, *Boundary-Layer*  
684 *Meteorology* 65 (1993) 159–179.
- 685 [8] M. Best, A model to predict surface temperatures, *Boundary-Layer*  
686 *Meteorology* 88 (1998) 279–306.
- 687 [9] M. Best, P. Cox, D. Warrilow, Determining the optimal soil temper-  
688 ature scheme for atmospheric modelling applications, *Boundary-layer*  
689 *meteorology* 114 (2005) 111–142.
- 690 [10] T. T. Chow, H. Long, H. Mok, K. Li, Estimation of soil temperature  
691 profile in hong kong from climatic variables, *Energy and Buildings* 43  
692 (2011) 3568–3575.
- 693 [11] B. K. Diefenderfer, I. L. Al-Qadi, S. D. Diefenderfer, Model to predict  
694 pavement temperature profile: development and validation, *Journal of*  
695 *Transportation Engineering* 132 (2006) 162–167.
- 696 [12] W. R. Herb, B. Janke, O. Mohseni, H. G. Stefan, Ground surface tem-  
697 perature simulation for different land covers, *Journal of Hydrology* 356  
698 (2008) 327–343.
- 699 [13] Å. Hermansson, Mathematical model for calculation of pavement tem-  
700 peratures: comparison of calculated and measured temperatures, *Trans-*  
701 *portation Research Record: Journal of the Transportation Research*  
702 *Board* (2001) 180–188.

- 703 [14] D. Ho, A soil thermal model for remote sensing, *IEEE transactions on*  
704 *geoscience and remote sensing* (1987) 221–229.
- 705 [15] C. Jacovides, G. Mihalakakou, M. Santamouris, J. Lewis, On the ground  
706 temperature profile for passive cooling applications in buildings, *Solar*  
707 *energy* 57 (1996) 167–175.
- 708 [16] J. Lin, On the force-restore method for prediction of ground surface  
709 temperature, *Journal of Geophysical Research: Oceans* 85 (1980) 3251–  
710 3254.
- 711 [17] G. Mihalakakou, M. Santamouris, J. Lewis, D. Asimakopoulos, On the  
712 application of the energy balance equation to predict ground tempera-  
713 ture profiles, *Solar Energy* 60 (1997) 181–190.
- 714 [18] G. Mihalakakou, On estimating soil surface temperature profiles, *Energy*  
715 *and Buildings* 34 (2002) 251–259.
- 716 [19] H. Nowamooz, S. Nikoosokhan, J. Lin, C. Chazallon, Finite difference  
717 modeling of heat distribution in multilayer soils with time-spatial hy-  
718 drothermal properties, *Renewable Energy* 76 (2015) 7–15.
- 719 [20] O. Ozgener, L. Ozgener, J. W. Tester, A practical approach to predict  
720 soil temperature variations for geothermal (ground) heat exchangers ap-  
721 plications, *International Journal of Heat and Mass Transfer* 62 (2013)  
722 473–480.
- 723 [21] Z. Qin, P. Berliner, A. Karnieli, Numerical solution of a complete surface  
724 energy balance model for simulation of heat fluxes and surface temper-

- 725       ature under bare soil environment, *Applied mathematics and computa-*  
726       tion 130 (2002) 171–200.
- 727 [22] H. Saito, J. Simunek, Effects of meteorological models on the solution of  
728       the surface energy balance and soil temperature variations in bare soils,  
729       *Journal of Hydrology* 373 (2009) 545–561.
- 730 [23] H. Swaid, M. E. Hoffman, The prediction of impervious ground surface  
731       temperature by the surface thermal time constant (sttc) model, *Energy*  
732       and *Buildings* 13 (1989) 149–157.
- 733 [24] M. Musy, L. Malys, B. Morille, C. Inard, The use of solene-microclimat  
734       model to assess adaptation strategies at the district scale, *Urban Climate*  
735       14 (2015) 213–223.
- 736 [25] J. Palyvos, A survey of wind convection coefficient correlations for build-  
737       ing envelope energy systems’ modeling, *Applied Thermal Engineering*  
738       28 (2008) 801–808.
- 739 [26] T. Defraeye, B. Blocken, J. Carmeliet, Convective heat transfer co-  
740       efficients for exterior building surfaces: Existing correlations and cfd  
741       modelling, *Energy Conversion and Management* 52 (2011) 512–522.
- 742 [27] W. H. McAdams, *Heat transmission*, 3rd, New York (1954).
- 743 [28] B. Morille, ÉLABORATION D’UN MODÈLE DU CLIMAT DIS-  
744       TRIBUÉ À L’ÉCHELLE DE L’ABRI ET DE LA PLANTE EN CUL-  
745       TURES ORNEMENTALES SOUS SERRES: ANALYSE DES TRANS-  
746       FERTS DE MASSE ET DE CHALEUR, BILANS ÉNERGÉTIQUES,  
747       Ph.D. thesis, Agrocampus-Centre d’Angers, 2012.



- 748 [29] J. Taine, J.-P. Petit, R. Séméria, J.-P. Petit, Transferts thermiques:  
749 mécanique des fluides anisothermes: cours et données de base, Dunod,  
750 1989.
- 751 [30] L. Malys, Évaluation des impacts directs et indirects des façades et des  
752 toitures végétales sur le comportement thermique des bâtiments, Ph.D.  
753 thesis, PhD thesis] Ecole Centrale de Nantes (France), 2012.
- 754 [31] P. Mestayer, J. Rosant, F. Rodriguez, J. Rouaud, The experimental  
755 campaign fluxsap 2010: climatological measurements over a heteroge-  
756 neous urban area, Int Assoc Urb Climate 40 (2011) 22–30.